Proceedings of the Korean Nuclear Society Spring Meeting
Kwangju, Korea, May 2002

Local Failure Characteristics of a Nuclear Reactor Pressure Vessel Nozzle under Severe Accident Conditions

Young J. Oh*, Kwang J. Jeong, and Il S. Hwang

Department of Nuclear Engineering, Seoul National University
San 56-1 Shinlim-dong, Gwanak-gu
Seoul, 151-742, Korea

Abstract

Most past studies for the creep rupture of a nuclear reactor pressure vessel (RPV) lower head under severe accident conditions, have focused on global deformation and rupture modes. Limited efforts were made on local failure modes associated with penetration nozzles as a part of TMI-2 Vessel Investigation Project (TMI-2 VIP) in 1990's. However, it was based on an excessively simplified shear deformation model. In the present study, the mode of nozzle failures is investigated using data and nozzle materials from Sandia National Laboratory's Lower Head Failure Experiment (SNL-LHF). Crack-like separations were revealed at the nozzle weld metal to RPV interfaces indicating the importance of normal stress component rather than the shear stress in the creep rupture. Creep rupture tests were conducted for nozzle and weld metal materials, respectively, at various temperature and stress levels. Stress distribution in the nozzle region is calculated using elastic-viscoplastic finite element analysis (FEA) using the measured properties. Calculation results are compared with earlier results based on the pure shear model of TMI-2 VIP. It has been concluded from both LHF-4 nozzle examination and FEA that normal stress at the nozzle/lower head interface is the dominant driving force for the local failure with its likelihood significantly greater than previously assumed.
Keywords : creep rupture, severe accident, nozzle ejection, elastic-viscoplastic finite element analysis, TMI-2 Vessel Investigation Project

1. Introduction

Three Mile Island Nuclear Power Plant Unit 2 (TMI-2) underwent a severe accident by

melting one half of its 120 ton core, as a results of reactor water drainage through a stuck-open PORV of the pressurizer and core uncover for two to four hours from the reactor trip [1]. Later it was found that about 19 tons of molten core or corium materials including structural metals and fuel ceramics began migrating downward to accumulate on the RPV lower head which prompted the inner wall temperature of RPV lower head to increase up to 1127 °C and to hold at the temperature for at least 30 minutes [2]. Due to the high temperature combined with high internal pressure (5~15 MPa), creep rupture of the RPV lower head was conceivable. Figure 1 [3] shows the postulated end-state configuration of the reactor vessel and the core.

Since the TMI-2 accident, the creep rupture behavior of RPV lower head under severe accident conditions has been extensively studied in order to predict the failure time.[1-4] Most of these studies, however, have been focused on global deformation and resultant rupture mode. As shown in Figure 2, nozzles are not welded through full thickness, and these regions can be expected to have higher stresses. Limited studies were made on the local failure mode associated with penetration nozzles as a part of TMI-2 Vessel Investigation Project (TMI-2 VIP) in 1990's [1]. The nozzle ejection, however, was concluded to be unlikely, primarily based on a greatly simplified model for pure shear mode of failure that is yet to be verified.

In this study, the mode and likelihood of nozzle failures are examined, by both experimental and analytical efforts. First, the tested vessel of Sandia National Laboratory's Lower Head Failure (LHF-4) Experiment (SNL-LHF) was examined, and creep rupture tests of nozzle and weld metal material were conducted at various temperature and stress ranges. Then, stress distribution in the nozzle region is calculated using elastic-viscoplastic finite element analysis (FEA) using material properties determined by mechanical test results. Finally, we define failure characteristics of the nozzle weld region, and propose a failure prediction model for nozzle weld region of RPV lower head under severe accident conditions.

2. Past Studies for RPV Nozzle Failure

TMI-2 Vessel Investigation Project (TMI-2 VIP) in 1990's [1] led to wide range of studies including relocation behavior of molten core, reactor internal pressure and temperature history, temperature distribution and creep deformation of RPV, modes of penetration nozzle region failure, etc.. As a part of nozzle failure analysis, nozzle ejection was considered. Figure 3 shows the effective stress analysis in the nozzle weld region. It was assumed that weld failure was due to shear stress resulted from internal pressure. From this assumption, the effective stress in the nozzle region was calculated, as follows.[3]

$$\tau_w = \frac{p_i \pi r_0^2}{2\pi r_0 L_w} = \frac{p_i r_0}{2L_w} \qquad \text{..... (1)}$$

$$\sigma_e = \sqrt{3}\tau_w \qquad \text{..... (2)}$$

where, τ_w, p_i, r_0, L_w and σ_e are shear stress, internal pressure, outer radius of nozzle, weld thickness and effective stress in the nozzle/weld boundary, respectively. This model does not take into account the normal stress arising from RPV hoop stress or stress concentration on notch tip

in the triple boundary of nozzle/weld/RPV base metal. No experimental validation was made to justify the shear failure model.

Later, Chu et al. of Sandia National Laboratory conducted a Lower Head Failure Experimental program (SNL-LHF) using 1/5 scale of TMI-2 RPV lower head. [4] Figure 4 shows the experimental apparatus of SNL-LHF. This program consisted of a series of eight experiments that were designed to examine the effects of spatial temperature/heat flux distribution, pressure, and reactor vessel structure elements and construction features on RPV deformation and failure. The fourth and fifth tests, LHF-4 & 5, included the nozzle weld in scaled test vessels. In LHF-4 experiment, penetration nozzle led to a failure at the weld/vessel interface. Expansion of penetration holes was found to be significant. Detailed measurement of deformation around the failed nozzle was not made..

3. Mechanical Property Measurements

Several researchers have performed the mechanical property measurements primarily on base metals to construct a database for lower head failure predictions. [1,3,4] However, the mechanical property database of weld metals has been insufficient to analyze the nozzle failure. In this study, tensile and creep tests of Alloy 690 nozzle material and Inco-82 weld metal were conducted at various temperature and stress levels. For tests at high temperature condition, an inductive heater and a servo-hydraulic testing machine with 10 tons capacity were used. Figure 4 shows the experimental apparatus of creep and tensile tests. Tensile and creep rupture tests were conducted using round bar type specimens as shown in Figure 5, according to ASTM E21-92, E8M00b [5, 6] and ASTM E139-00 [7], respectively. In high temperature tensile and creep tests, strains were determined by LVDT attached in actuator.

Stress-strain curves of nozzle and weld materials are shown in Figure 6 (a) and (b), respectively. The yield strength and tensile strength of nozzle materials are very close to those of weld materials, and nozzle materials have larger elongation than weld metal except at 500 °C. Tensile and yield strength of nozzle and weld materials were compared with those of SA508Cl.3 RPV steel [8] in Figure 7 (a) and (b). At temperature range below 500 °C, the nozzle and weld materials have lower yield strength than SA508Cl.3 RPV steel and all the three materials have almost the same tensile strength. At temperature above 600 °C, the nozzle and weld materials have higher yield strength and tensile strength than RPV steel.

High temperature creep tests were conducted at 760 °C, 870 °C and 980 °C, respectively. All the specimens were tested in constant load condition at three initial stress levels at a given temperature. Figure 8 shows Larson-Miller Parameter (LMP) [9] of nozzle and weld materials. Nozzle materials show higher creep strength than weld materials.

Because of its wide acceptance in elastic visco-plastic finite element analysis [10], the minimum creep rate of each creep test specimens was determined, as shown in Figure 9. Minimum creep rate means the time rate of the steady-state creep strain during the secondary creep region. Measured minimum creep rates of nozzle and nozzle weld materials, are shown in Figure 10. As a result, elastic, plastic and creep database for nozzle and weld metals was

constructed and was used in the analysis of the nozzle failure to be described herein.

4. Destruction Examination of SNL-LHF Vessel

The LHF-4 vessel from SNL-LHF was destructively examined. Figure 11 shows the inner surface of LHF-4 vessel, where a crack is observed at the boundary of RPV vessel and weld metal. To confirm the exact position of the crack, the cross-section area and cutting direction, shown in Figure 11, were observed. Figure 12 shows the cross-section of the nozzle weld region of LHF-4. Shear deformation due to internal pressure was found to be insignificant. In contract, the normal direction deformation was predominant.

The nozzle through-hole was expanded due to global creep which dilated the weld joined region of the nozzle. A crack was initiated at the boundary of weld metal and RPV base metal, and we point out that recent studies for weld heat affected zone show lower creep strength [12~14]. The nature of the crack was not mode II (shearing mode) but mode I (opening mode). From the result, it can be concluded that the most important failure mode for TMI-2 accident is the separation of the weld metal by normal stress whereas the previously assumed shear mode is unimportant.

5. Finite Element Analysis

To understand stress distribution in nozzle weld region, elastic-viscoplastic finite element analysis was conducted using the measured mechanical properties. For finite element analysis, the creep data set was fitted with Bailey-Norton type equation, as shown in Figure 13 (a) and (b). The Bailey-Norton type equation is then expressed, as follows ;

$$\dot{\varepsilon} = A\sigma^{m} \exp\left(-\frac{B}{T}\right) \quad \cdots\cdots\cdots (3)$$

where $\dot{\varepsilon}$, σ, T, A, B and m are minimum creep rate, applied stress, temperature and fitting constants, respectively. The finite element analysis was conducted using ABAQUS Standard version 5.8. [15]

In order to examine the validity of TMI-2 VIP nozzle model of Eq. (1) and (2), two types of boundary conditions were used as shown in Figure 14. The model of (a) of Figure 14 is similar to shearing approximation employed in TMI-2 VIP. The model (b) corresponds to our new model developed to allow for generalized loading conditions for the case of APR1400 (Advanced Power Reactor 1400) with internal pressure of 1 MPa. Figure 15 shows the distribution of each stress component in the nozzle weld region. Each direction of stress component and the definition of “distance from notch tip” are shown in Figure 14 (a). Figure 15 (a) shows the result of model (a) of Figure 14, and interfacial shear stress (s12) has similar values with normal stress (s11 and s33). But, in the model (b) of Figure 14, shear stress shows the negligible value compared with normal stress as shown in Figure 15 (b). Normal stress of model (a) is much smaller than that of model (b).

With this geometry and internal pressure condition, the TMI-2 VIP shear model of Eq. (1) and (2) predict 0.87 MPa of the average effective stress. Figure 16 shows the effective stress distributions of model (a) and model (b) of Figure 14. The computation results of model (a) of Figure 14, that is FEA model of TMI-2 VIP shear model, agree well with hand calculation result of TMI-2 VIP of Eq. (1) and (2). But, effective stress of model (a) of Figure 14 is much smaller than that of model (b) of Figure 14. Therefore, the earlier TMI-2 VIP model is shown to underestimate the applied stress of nozzle weld under severe accident condition.

To understand deformation and failure characteristics of nozzle weld, the LHF-4 experiment was analyzed. In Figure 17, the analysis result was compared with experimental data for global deformation behavior of RPV lower head. Analysis result agreed well with experimental data. Figure 18 shows the local deformation behavior of nozzle weld region. RPV hole expansion and notch tip deformation was normalized using final displacement value in Figure 18 (a). From Figure 18 (a) the local deformation behavior determined by notch tip deformation appears different from global deformation behavior that is represented by vertical displacement of RPV and hole expansion. Figure 18 (b) shows, however, that this difference is due to thermal expansion and local deformation behavior is similar with global deformation behavior in a view point of creep deformation without thermal expansion.

To confirm these characteristics of local deformation behavior in nozzle weld region, the deformation behavior of two cases are compared as shown in Figure 19 (a) and (b). Figure 20 shows that hole expansion of nozzle excluded model agree well with prototype model. It means that existence of nozzle weld does not affect the hole expansion, and the notch tip deformation is controlled primarily by hole expansion. This indicates that the nozzle failure process is not load controlled but displacement controlled. Therefore we can simulate the evolution of through-wall crack using a notched bar specimen under the displacement control as shown in Figure 21 provided that biaxial tensile stress effect can be neglected.

6. Conclusions

From the study of local failure mode of a nuclear reactor pressure vessel nozzle under severe accident conditions, the following conclusions are made.

1) The tensile and creep properties database was constructed for nozzle and nozzle weld materials under severe accident condition.
2) The nozzle weld region of LHF-4 vessel was examined after testing at SNL.
   - Global RPV hoop load induced the crack initiation and propagation.
   - Fracture initiation site is the boundary of RPV and weld metal.
3) Elastic-viscoplastic finite element analysis was made.
   - TMI-2 VIP model underestimates the effective stress because the hoop stress was excluded.
   - Notch tip deformation behavior is in a good consistency with global deformation behavior of vessel lower head.
   - The nozzle failure is not load controlled but displacement controlled.
4) A notched-bar tensile test method is proposed for the nozzle failure predictions under

severe accidents.

Acknowledgement

The authors would like to express their deep gratitude for Dr. T. Y. Chu of SNL and Dr. H. D. Kim of Korea Atomic Energy Research Institute for providing LHF-4 vessel through a collaboration program coordinated by Dr. A. Behbahani of U.S. NRC. We also would like to thank Professor K. B. Yoon of Chung Ang University for helpful comments. This work was financially supported by Korea Atomic Energy Research Institute through Korea Institute Science and Technology Evaluation and Planning.

Reference

[1] L. A. Stickler et al., Calculation to Estimate the Margin to Failure in the TMI-2 Vessel, NUREG/CR-6196, TMI V (93)EG01, EGG-2733, March 1994.
[2] OECD, Three Mile Island Reactor Pressure Vessel Investigation Project, Proc. Of an open forum sponsored by the OECD NEA and USNRC, 1994.
[3] J. L. Rempe et al., Light Water Reactor Lower Head Failure Analysis, NUREG/CR-5642, 1993.
[4] T. Y. Chu et al., Lower Head Failure Experiments and Analyses, NUREG/CR-5582, Sandia National Laboratories, 1999.
[5] ASTM E21-92, Standard Test Methods for Elevated Temperature Tension Tests of Metallic Materials, Annual Book of ASTM Standards Vol. 03.01, 2001
[6] ASTM E8M, Standard Test Methods for Tension Testing of Metallic Materials, Annual Book of ASTM Standards Vol. 03.01, 2001
[7] ASTM E139-96, Standard Test Methods for Conducting Creep, Creep-Rupture, and Stress-Rupture Tests of Metallic Materials, Annual Book of ASTM Standards Vol. 03.01, 2001
[8] D. C. Lim, Study on the Creep Behavior of SA508Cl.3 at Elevated Temperature, Master thesis, Seoul National University, 1998.
[9] F.R. Larson, and J. Miller, A time-temperature relationship for rupture and creep stress, Trans. ASME, July 1952, pp756-775.
[10] K. J. Jeong, A Dimensionless Modeling Approach for the Elastic-Viscoplastic Deformation of Nuclear Reactor Vessels, Ph. D. thesis, Seoul National University, 2001.
[11] M.J. Driscoll et al., U.S. Patent No. 4113560
[12] K. Laha et al., Prediction of creep deformation and rupture behaviour of 2.25Cr-1Mo weld joint, International Journal of Pressure Vessel and Piping, Vol. 77, pp761-769, 2000.
[13] Y. Otoguro et al., Creep rupture strength of heat affected zone for 9Cr ferritic heat resisting steels, Nuclear Engineering and Design, Vol. 196, 2000.
[14] S.C. Tjong, et al., Microstructural characteristics and creep rupture behavior of electron beam and laser welded AISI 316L stainless steel, Journal of Nuclear Materials, Vol. 227, pp24-31, 1995.
[15] Hibbit, Karlsson & Sorensen, Inc., ABAQUS user's manual, Ver. 5.8, Providence, Rhode Island, 1998.

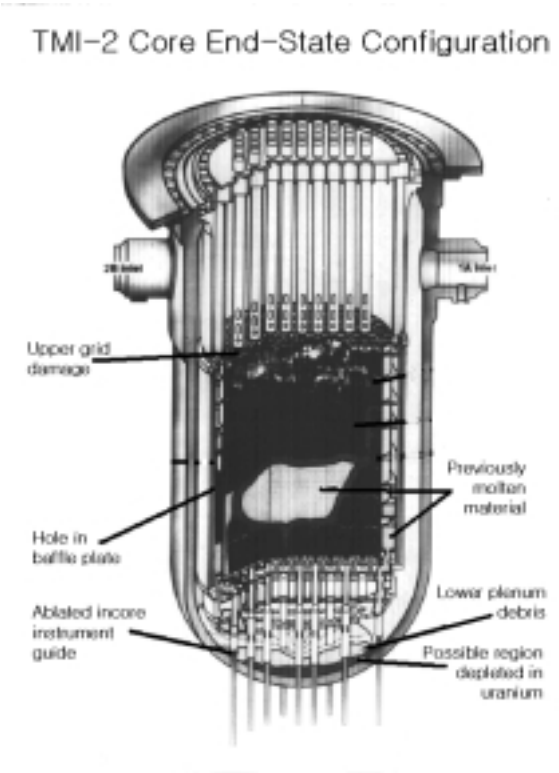

Figure 1. TMI-2 core end-state configuration. [7]

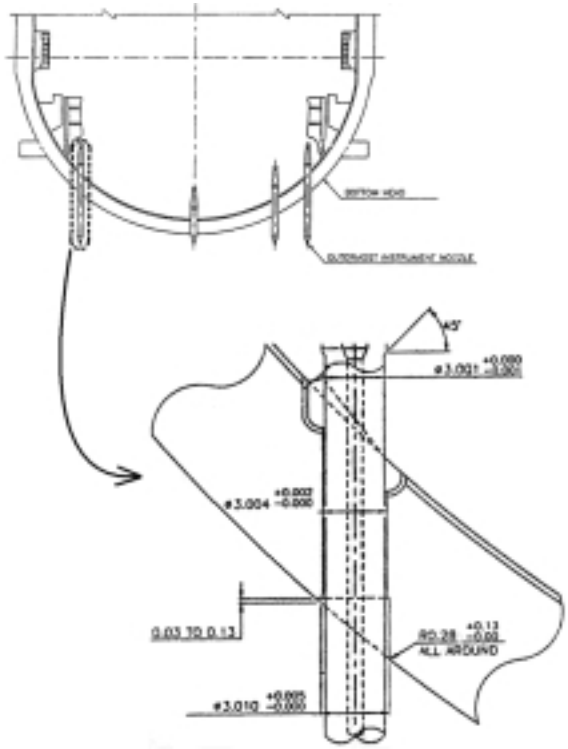

Figure 2. Nozzle weld region of RPV lower head for KSNPP (dimension in inch).

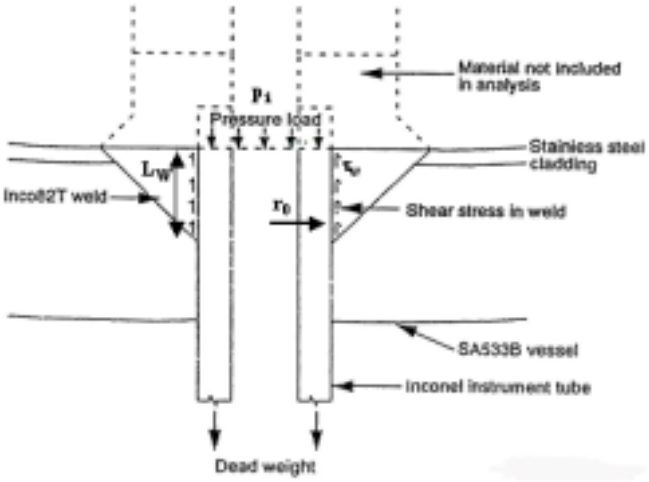

Figure 3. Schematic diagram of nozzle weld region for calculating effective stress assuming pure shear mode of failure [1]

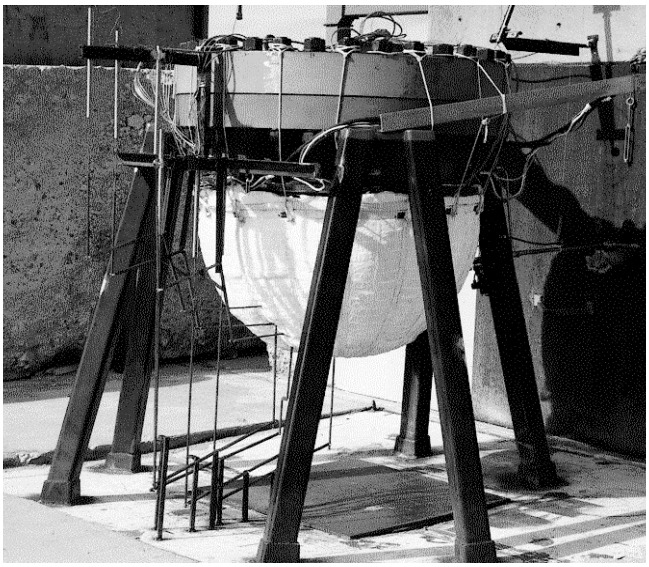

Figure 3. Sandia National Lab. Lower Head Failure experiments (SNL-LHF). [4]

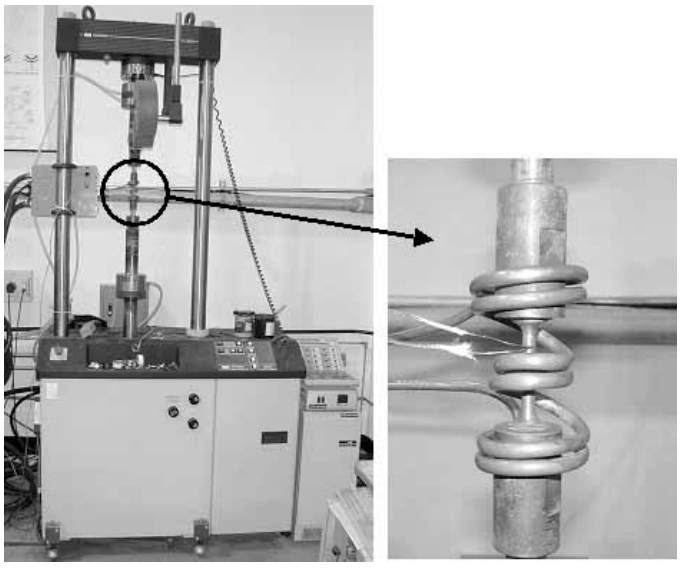

Figure 4. Experimental apparatus nozzle and weld metal creep tests in this work

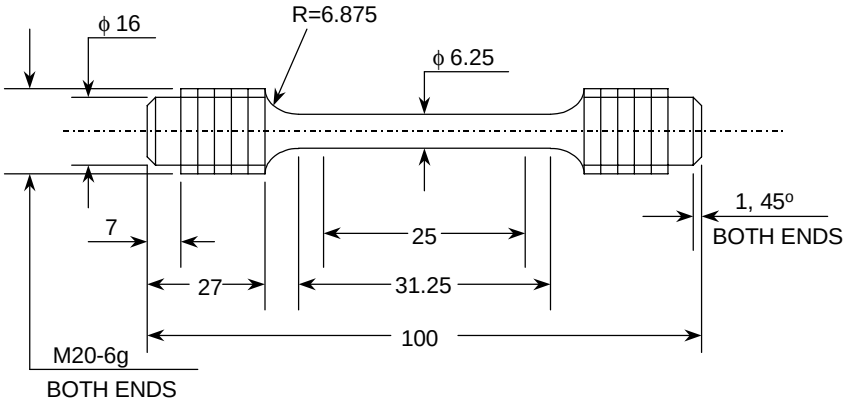

Figure 5. Specimen design for tensile and creep tests.

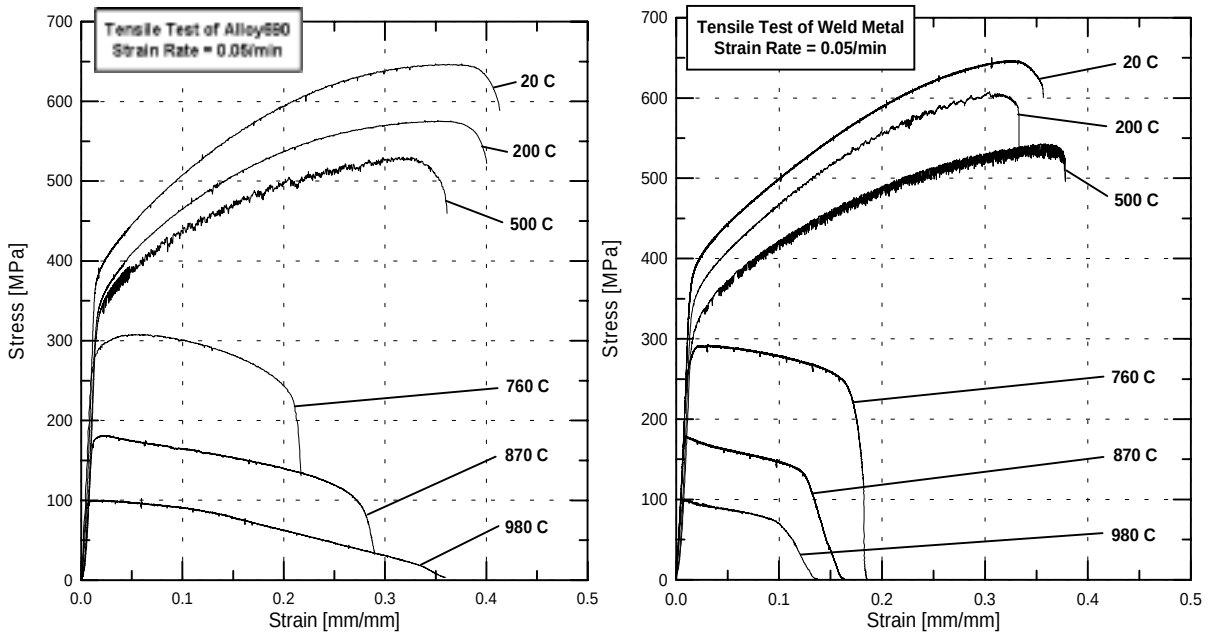

(a) Alloy 690, nozzle material (b) I-82 filer wire, nozzle welding material

Figure 6. Stress-strain curves of nozzle and weld materials under tensile loading conditions

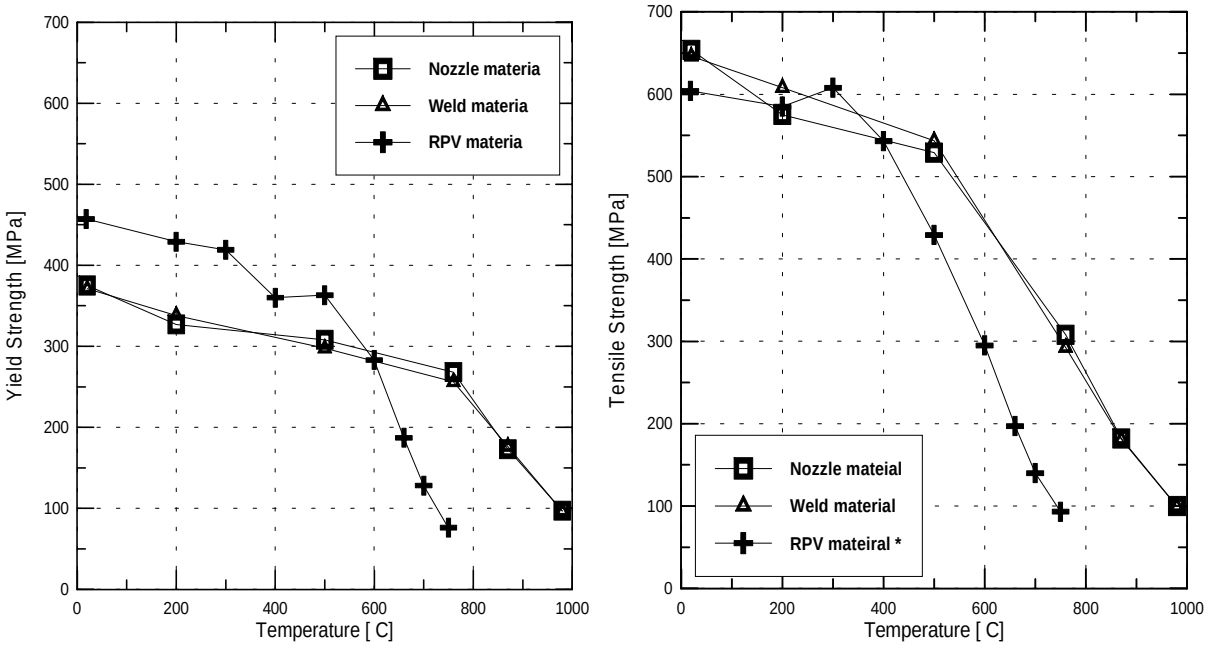

(a) Yield strength (b) Tensile strength

Figure 7. Yield strength and tensile strength of nozzle and weld materials as function of temperature.

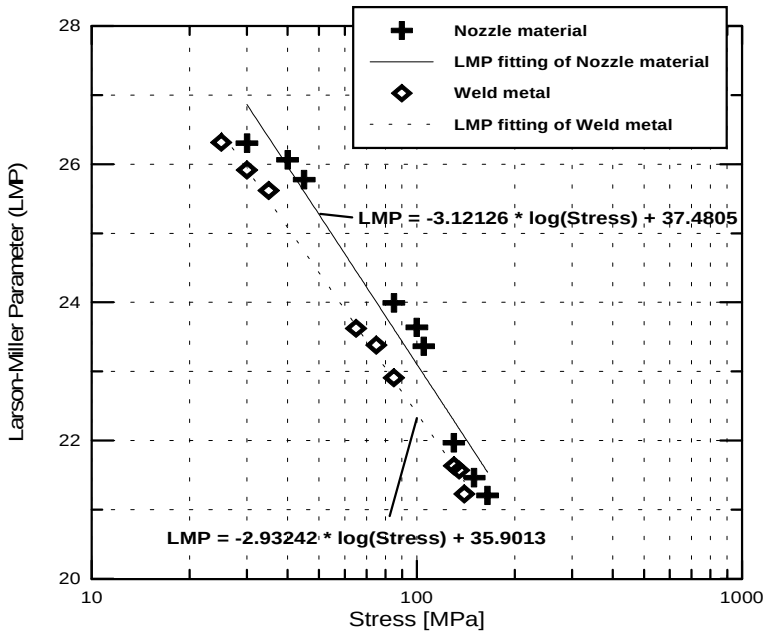

Figure 8. Larson-Miller Parameter (LMP) of nozzle and weld materials

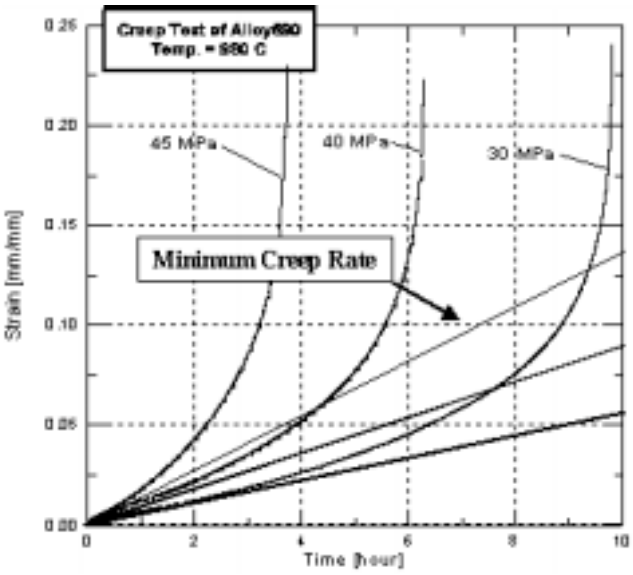

Figure 9. Minimum creep rate of Alloy690 tested at 980 °C

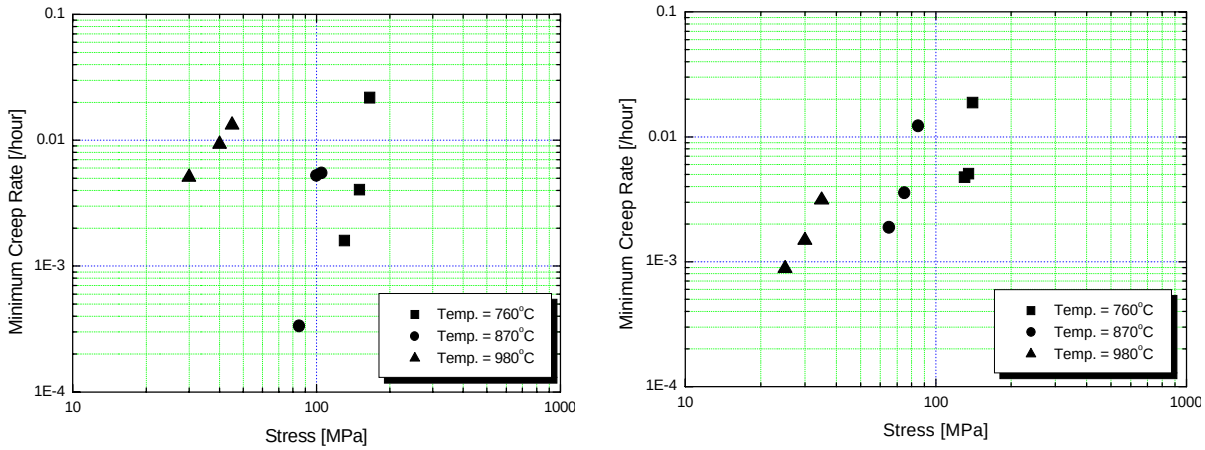

(a) Alloy690, nozzle material (b) Inco-82, nozzle weld metal

Figure 10. Measured minimum creep rates of nozzle and weld metal as a function of initial stress.

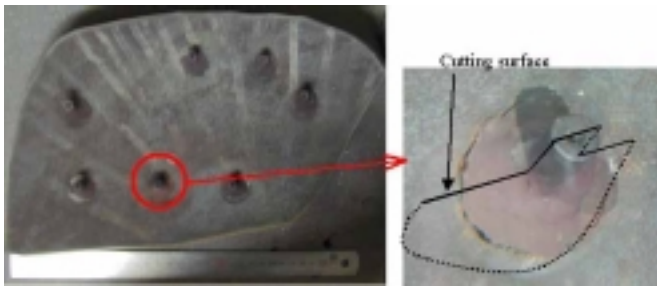

Figure 11. Inner surface of LHF-4 tested vessel and cutting direction for observing cross-section area

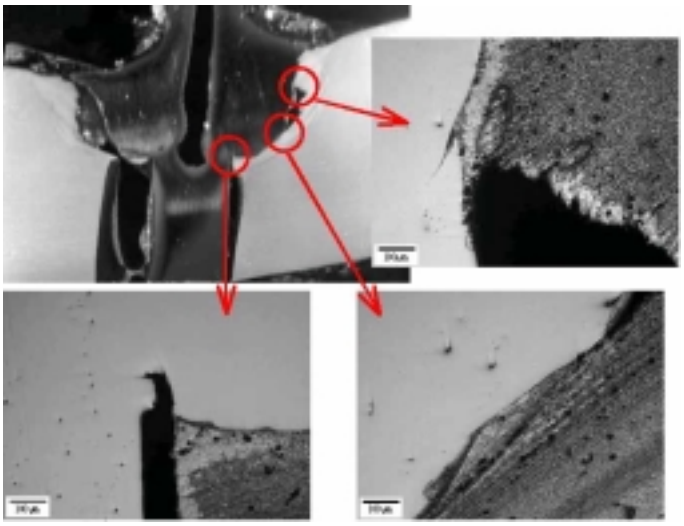

Figure 12. Cross-section photomicrographs of LHF-4 vessel tested at Sandia National Laboratory.

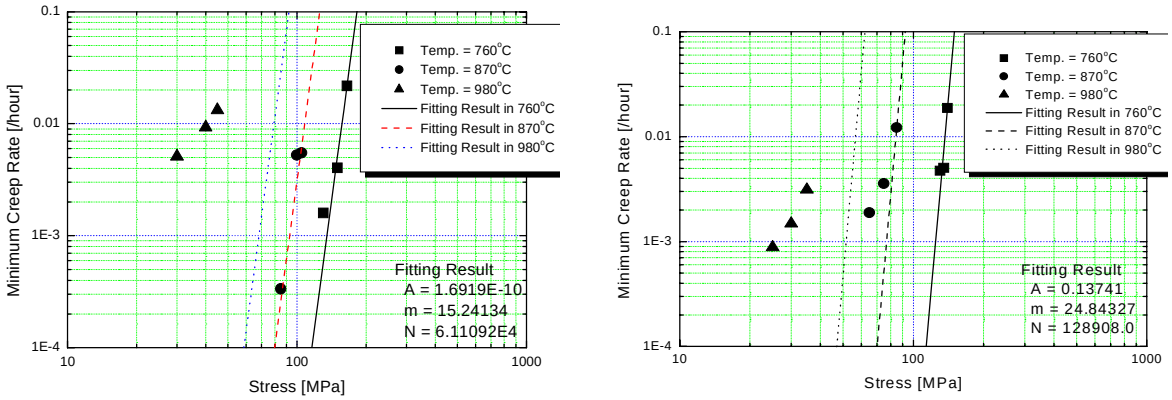

(a) Alloy690, Nozzle material (b) I-82, weld material

Figure 13. Least square fits of minimum creep rate of nozzle and weld materials into Bailey-Norton equation.

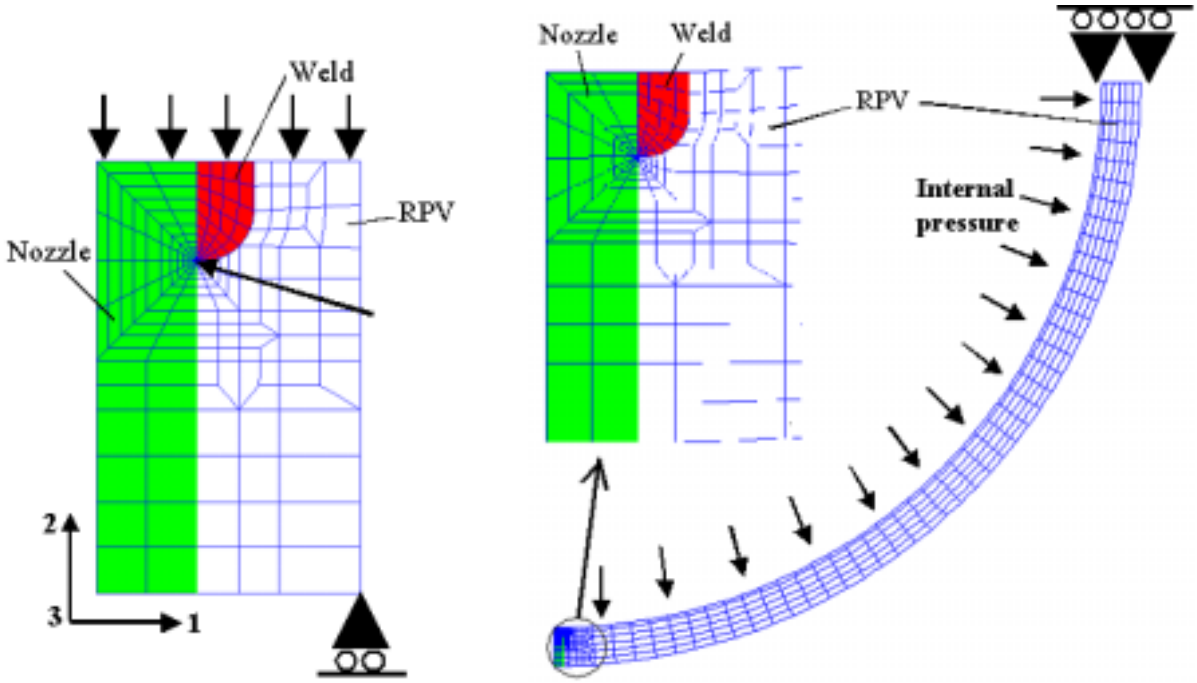

(a) TMI-2 VIP model case (b) Generalized nozzle model

Figure 14. Finite element analysis modeling for comparison of TMI-2 VIPshear model with generalized nozzle model

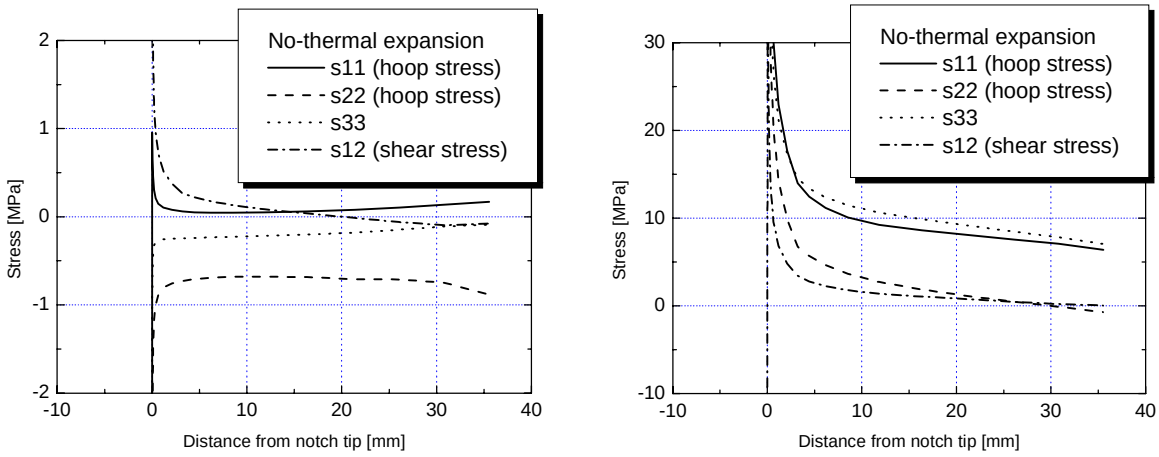

(a) No-spherical vessel (TMI-2 VIP shear model case)

(b) With spherical vessel (generalized nozzle model case)

Figure 15. Distribution of each stress components in nozzle weld region.(s11, s22, s33 denotes normal stress in the direction 1, 2, 3, respectively, defined in Fig. 14. s12 denotes shear stress on plane 1 in direction 2)

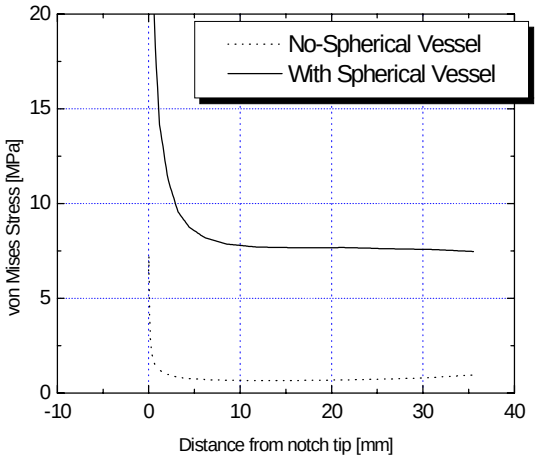

Figure 16. Distribution of von Mises stress.

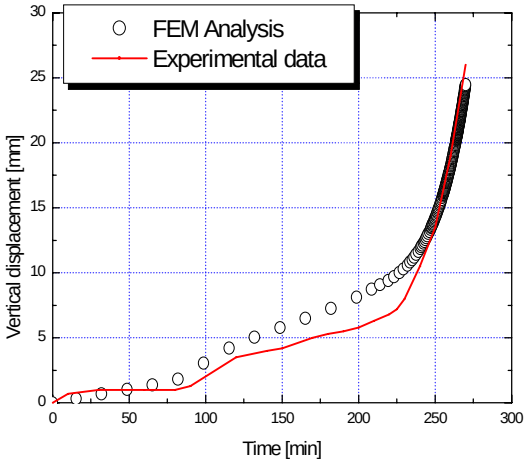

Figure 17. Validation of finite element model using SNL LHF-4 experiment.

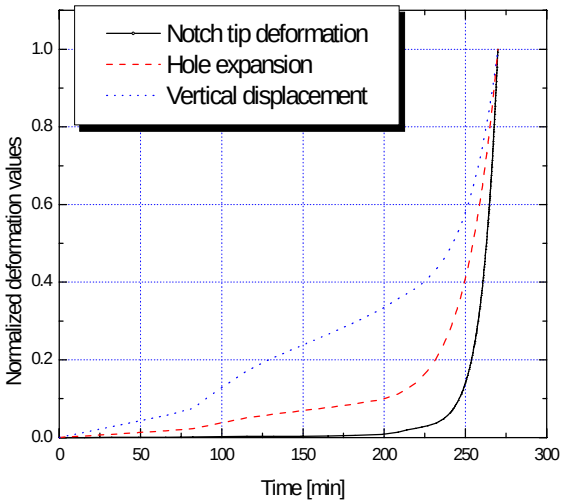

(a) Include thermal expansion

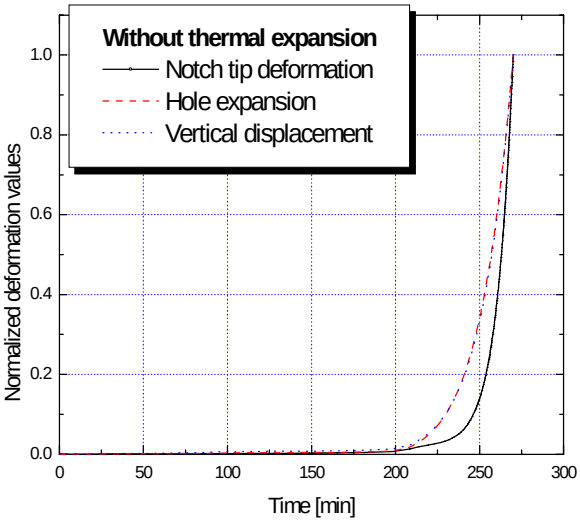

(b) exclude thermal expansion

Figure 18. Deformation behavior of LHF-4 vessel nozzle as function of testing time. (Deformation has been normalized by maximum deformation at end)

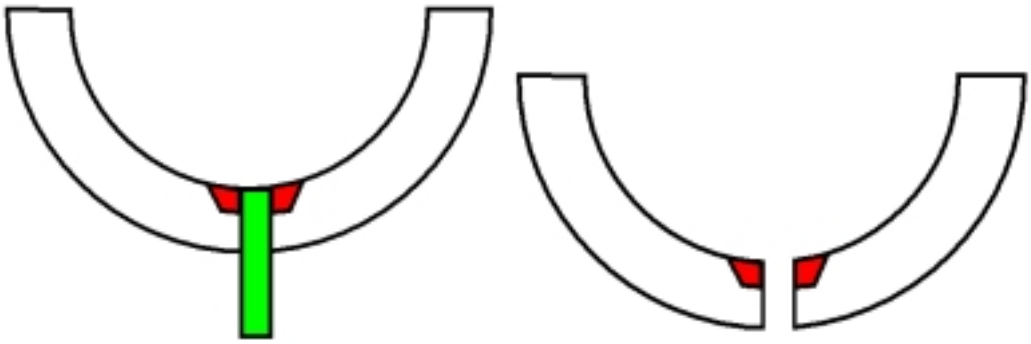

(a) Prototype model. (b) Nozzle excluded model.

Figure 19. RPV lower head models for understanding nozzle weld region characteristics.

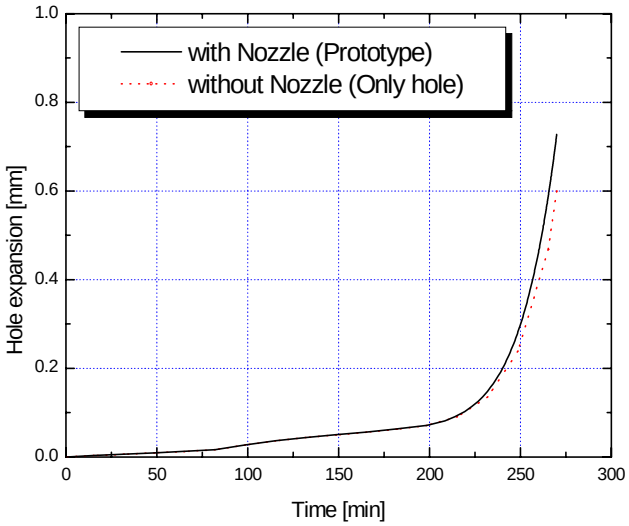

Figure 20. Hole expansions of prototype model and nozzle excluded model.

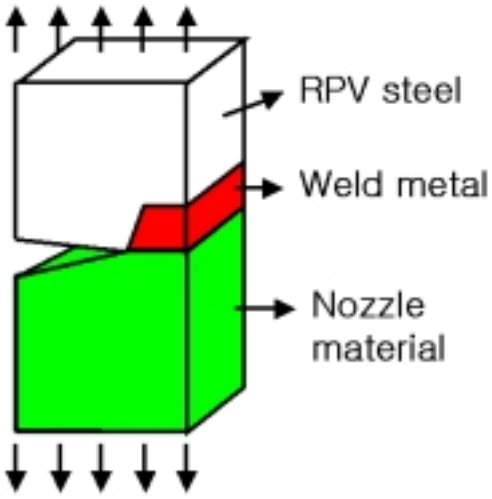

Figure 21. Proposed tensile type creep test method using a notched bar weld specimen to predict through-wall cracking.